ChemComm

COMMUNICATION

View Article Online
View Journal | View Issue

Check for updates

Cite this: *Chem. Commun.*, 2021, 57, 6039

Received 30th March 2021,
Accepted 17th May 2021

DOI: 10.1039/d1cc01881g

rsc.li/chemcomm

Published on 17 May 2021. Downloaded by Izmir Yuksek Teknoloji on 9/6/2022 2:34:58 PM.

BODIPY–vinyl dibromides as triplet sensitisers for photodynamic therapy and triplet–triplet annihilation upconversion†

Suay Dartar,[a] Muhammed Ucuncu,[b] Erman Karakus,[c] Yuqi Hou,[d] Jianzhang Zhao *[d] and Mustafa Emrullahoglu *[e]

We devised a new generation of halogen-based triplet sensitisers comprising geminal dibromides at the vinyl backbone of a BODIPY fluorophore. Incorporating geminal dibromides into the π-conjugation of BODIPY enhanced intersystem crossing due to the heavy atom effect, which in turn improved the extent of excited triplet states.

Thanks to recent advancements, photodynamic therapy has established itself as a safe, reliable clinical modality for treating localised cancers,[1a] dermatological diseases[1b] and several bacterial infections.[1c]

To mediate oxidative photodamage to living cells, PDT relies on the light-triggered generation of reactive oxygen species (*e.g.*, singlet oxygen) by photosensitisers. The modality's efficacy, determined by the interplay of the photosensitiser, light and molecular oxygen, depends heavily on the photosensitiser's capacity to generate singlet oxygen.[2]

Most photosensitisers investigated for clinical PDT comprise cyclic tetrapyrrolic structures inspired by naturally derived porphyrins such as haematoporphyrin.[3] Other than porphyrin-based photosensitisers, dipyrromethene-based (BODIPY) dyes, given their excellent photophysical properties, have emerged as highly promising candidates for photosensitisers not only for PDT but for bioimaging applications as well.[4] In fact, the unmodified BODIPY core (*e.g.*, tetramethyl-BODIPY) is utterly without effect in PDT, as it is deprived of excited triplet states, a photophysical parameter necessary for generating singlet oxygen.[5]

Nevertheless, recent studies on BODIPY-based photosensitisers have elegantly demonstrated the possibility of switching the excited state of a BODIPY dye from a singlet to a triplet state.[6]

Manipulating the BODIPY skeleton *via* halogenation,[7] first reported by Nagano *et al.*,[7c] is an effective approach to promoting the spin–orbital coupling (SOC) needed to observe triplet states. Integrating transition metals into the BODIPY skeleton,[6c,8] conjugating the core to poly/aromatics (*e.g.*, anthracene or fullerene),[9] incorporating donor groups to the core,[10] and orthogonal dimerisation[11] are other possible methods of improving a BODIPY dye's efficiency in generating singlet oxygen (Scheme 1).

Among these methods, installing halogens (*e.g.*, I or Br) is by far the most practical way to transform an inactive BODIPY dye into a highly active triplet sensitiser. However, the photoactivity of halogenated BODIPY is highly dependent on the type of halogen atom and the pattern of halogen substitution.[12] Because iodine exerts a greater heavy atom effect than bromine, iodinated BODIPY derivatives usually exhibit far greater singlet oxygen

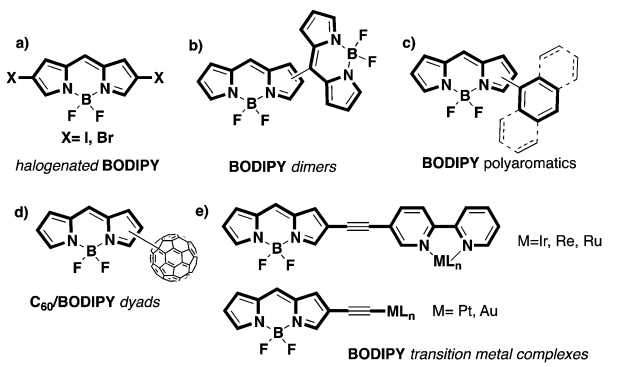

Scheme 1 BODIPY-based photosensitisers for singlet oxygen generation.

[a] Department of Chemistry, Faculty of Science, İzmir Institute of Technology, İzmir, Turkey
[b] Department of Analytical Chemistry, Faculty of Pharmacy, Izmir Katip Celebi University, Izmir, Turkey
[c] Organic Chemistry Laboratory, Chemistry Group, The Scientific & Technological Research Council of Turkey, National Metrology Institute (TUBITAK-UME), Kocaeli, Turkey
[d] State Key Laboratory of Fine Chemicals, School of Chemical Engineering, Dalian University of Technology, E 208 Western Campus, 2 Ling-Gong Road, Dalian 116012, P. R. China
[e] Department of Photonics, Faculty of Science, İzmir Institute of Technology, Urla, 35430, İzmir, Turkey. E-mail: mustafaemrullahoglu@iyte.edu.tr

† Electronic supplementary information (ESI) available. See DOI: 10.1039/d1cc01881g

Published on 17 May 2021. Downloaded by Izmir Yuksek Teknoloji on 9/6/2022 2:34:58 PM.

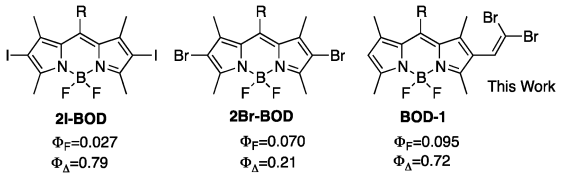

Scheme 2 Comparison of **BOD-1** with literature examples.

generation efficiency (Scheme 2). Although halogenation at the 2,6-positions is essential for triplet sensitisation, multiple halogenations do not always benefit the efficiency of generating singlet oxygen.[13] Given their high photoactivity, iodinated BODIPY dyes emit nearly no fluorescence, which renders them useless for fluorescence imaging applications.

By sharp contrast, brominated BODIPY dyes, despite having lower photoactivity, usually emit a faint fluorescence emission.[14]

For PDT today, the goal of developing a photosensitiser with a fine balance between fluorescence emission and singlet oxygen generation, a characteristic that is desirable for effective image-guided PDT, has galvanised considerable attention. Recent studies have even shown that BODIPY dyes can be conveniently used as platforms for theragnostic PDT.[14] Nevertheless, designing halogenated BODIPY-photosensitisers with both high efficiency in generating singlet oxygen and trackable fluorescence emission remains a significant challenge. Alternative synthetic routes to readily access halogenated BODIPY dyes with dual photonic action are thus in high demand.

With that need in mind, we devised a BODIPY construct as a potential new generation triplet photosensitiser with geminal dibromides at the vinyl backbone of a BODIPY core.

Building upon our previous investigation into transition metal-based BODIPY photosensitisers (Scheme 1e), we anticipated that placing heavy atoms, namely halogens, into the extended π-conjugation of the BODIPY skeleton would enhance the probability of ISC due to the heavy atom effect and, in turn, improve the possibility of observing excited triplet states (Scheme 2).[8b]

Herein, we present the design, synthesis and spectroscopic investigation of halogenated vinyl-BODIPY derivatives, denoted **BOD-1** and **BOD-2**, with high efficiency in generating singlet oxygen in solution and in living environments. Both compounds were prepared by following the synthetic route outlined in Scheme 3. The dibromo olefination (*e.g.*, Ramirez olefination)[15a] of 2-formyl-BODIPY with carbon tetrabromide and triphenylphosphine in dichloromethane at 0 °C gave **BOD-1** in a reasonable yield of approximately 35%. **BOD-2** was prepared from a 2,6-diformyl-BODIPY derivative following the same synthetic protocol.[15b,c]

The identity of both compounds was confirmed *via* nuclear magnetic resonance spectroscopy and high-resolution mass spectrometric analysis, consistent with reported data.[16] Nevertheless, the triplet-state properties of BODIPY-vinyl dibromides (*e.g.*, triplet photosensitisation capabilities, singlet- and triplet-state lifetimes, photocytotoxicity and TTA upconversion behaviours) remained unexplored. With this in mind, we closely examined the photophysical properties of **BOD-1** and **BOD-2** and their ability to generate singlet oxygen by performing steady-state fluorescence and absorption spectroscopy, while we investigated

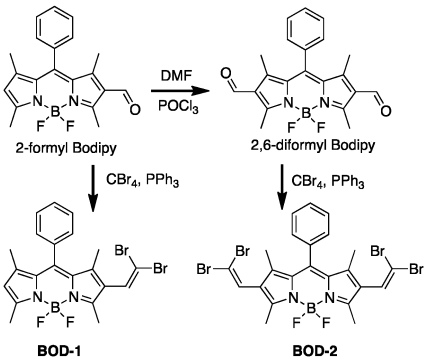

Scheme 3 Synthetic route for **BOD-1** and **BOD-2**.

their triplet-state characteristics by using nanosecond transient absorption spectroscopy.

Table 1 shows the electronic absorption and emission data of **BOD-1** and **BOD-2** and, for comparison, of the 2,6-dibromo and 2,6-diiodo-BODIPY derivatives.[17]

As illustrated in Fig. 1, the UV-visible spectra of **BOD-1** and **BOD-2** showed absorption bands in the range of 510–525 nm. The absorption band of **BOD-1** with a single dibromo-vinyl unit was centred at 513 nm, whereas incorporating the second dibromo-vinyl unit induced a moderate bathochromic shift to 525 nm, which clearly indicated a larger extension of the π-conjugation for compound **BOD-2** than that of **BOD-1**. Compared with the BODIPY derivative free of heavy atoms, **BOD-1**, upon excitation at 480 nm (5 μM), exhibited a red-shifted emission band at 533 nm, with a small fluorescence quantum yield (Φ_F = 0.095, τ_F = 1.41 ns). Similarly, upon excitation at 500 nm (5 μM), **BOD-2** exhibited a red shifted emission band at 552 nm (Φ_F = 0.11, τ_F = 1.50 ns).

The brief decay time of the excited singlet state, along with the low fluorescence quantum yield of both compounds, can be attributed to the efficiency of ISC from an excited singlet state to an excited triplet state *via* the heavy atom effect induced by the halogens linked to the BODIPY structures.

The population of the excited triplet states was confirmed by nanosecond time-resolved transient absorption spectroscopy (Fig. 2). With pulsed laser excitation at 355 nm, significant bleaching was observed at 510 nm and 520 nm for **BOD-1** and **BOD-2**, respectively, along with transient absorptions at 420 nm and 550–700 nm, which are typical characteristics of BODIPY

Table 1 Photophysical parameters of **BOD-1**, **BOD-2**, **2Br-BOD** and **2I-BOD**

Compound[a]	λ_{abs}	ε^b	λ_{em}	$\Phi_F{}^c$	$\tau_F{}^d$/(ns)	$\tau_T{}^d$/(μs)	$\Phi_\Delta{}^e$	$\Phi_{UC}{}^g$ (%)
BOD-1	513	8.9	533	0.095	1.41	145	0.72	1.39
BOD-2	525	9.3	552	0.110	1.50	101	0.64	4.88
2BrBOD[17]	538	4.1	569	0.070	—	—	0.21	—
2I-BOD[7c]	533	8.9	552	0.027[f]	0.13	57.1[f]	0.79	5.40[7d]

[a] In CH_2Cl_2 (5 μM). [b] Molar absorption coefficient at the absorption maximum, ε: 10^4 M^{-1} cm^{-1}. [c] Fluorescence quantum yield. [d] Fluorescence lifetimes. [e] Singlet oxygen ($^1O_2$) quantum yield. [f] In CH_3CN. [g] Upconversion quantum yields, with **2I-BOD** (Φ_F = 2.7% in CH_3CN) as the reference, and perylene as a triplet acceptor.

 This journal is © The Royal Society of Chemistry 2021

Published on 17 May 2021. Downloaded by Izmir Yuksek Teknoloji on 9/6/2022 2:34:58 PM.

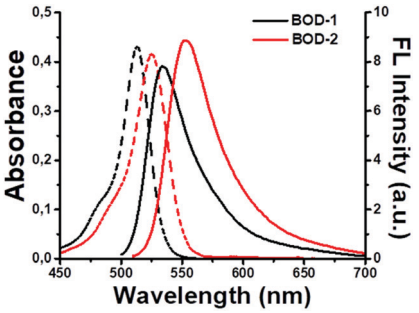

Fig. 1 UV-vis spectra of **BOD-1** (black dashed line) (5 μM) and **BOD-2** (red dashed line) (5 μM) in CH_2Cl_2 and emission spectra of **BOD-1** (black straight line) and **BOD-2** (red straight line) in CH_2Cl_2 (λ_{ex}: 480 nm for **BOD-1** and λ_{ex}: 500 nm for **BOD-2**).

based triplet sensitisers. The triplet-state lifetime of **BOD-1** (τ_T), at 101 μs was remarkably long, and **BOD-2**'s, at 145 μs, was even longer.

BODIPY-based organic triplet photosensitisers, particularly those bearing heavy atoms in the BODIPY skeleton, demonstrate outstanding potential for use in triplet–triplet annihilation upconversion,[18] a process in which harvested energy is transferred from a triplet sensitiser to an acceptor *via* triplet–triplet energy transfer (TTET), with the result of emission at higher energy. Bearing that dynamic in mind, we measured the TTA upconversion quantum yields of both **BOD-1** and **BOD-2** using perylene as the triplet acceptor (Fig. 3). Significant upconversion, peaking at 4.88%, was observed with **BOD-2** and perylene, whereas the yield for **BOD-1** was dramatically lower (Φ_{uc} = 1.39%), calculated with 2,6-diiodo-1,3,5,7-tetramethyl-8-phenyl-BODIPY (2I-BOD; Φ_F = 2.7% in CH_3CN).

Having unambiguously confirmed the triplet-state characteristic of both **BOD-1** and **BOD-2**, we next assessed their capabilities to generate singlet oxygen by employing an indirect trapping method using diphenyl isobenzofuran (DPBF) as a singlet oxygen scavenger. Singlet oxygen reacts with DPBF to yield 1,2-dibenzoylbenzene, and the extent of DPBF-related

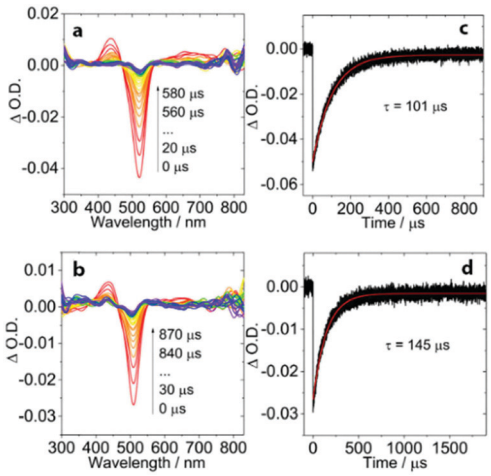

Fig. 2 Nanosecond transient absorption spectra of (a) **BOD-1** and (b) **BOD-2**; relative decay traces of (c) **BOD-1** at 510 nm and (d) **BOD-2** at 520 nm, measured in deaerated CH_2Cl_2, c = 10 μM, λ_{ex} = 355 nm.

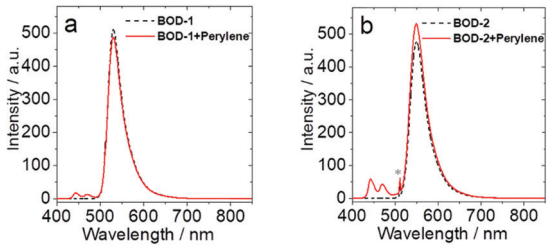

Fig. 3 TTA upconversion with (a) **BOD-1** and (b) **BOD-2** as the triplet photosensitisers (10 μM) and perylene as the triplet acceptor (10 μM) in deaerated dichloromethane, excited with a 510 nm cw-laser with a power density of 44.4 mW cm^{-2}. The asterisk in (b) indicates the scattered laser.

photodegradation was evaluated by measuring the decrease in DPBF's absorption band at 415 nm (Fig. S1, ESI†).[19]

The photodegradation of DPBF was evaluated under light irradiation using a green LED source at a distance of 15 cm from the cuvette window (525 nm, 3.3 mW cm^{-2}). Among the results, the absorption band of DPBF at 415 nm decreased sharply and had disappeared entirely within a couple of minutes, which clearly indicates the high efficiency of both compounds in generating singlet oxygen. The best decay in absorption was observed in CH_2Cl_2, among other solvent systems. The efficiency of generating singlet oxygen, known as singlet oxygen quantum yield, had a remarkably high Φ_Δ value (**BOD-1**; Φ_Δ = 0.72% and **BOD-2**; Φ_Δ = 0.64%), calculated with **2I-BOD** as the reference (Table 1). Moreover, using light irradiation (525 nm, 10 mW cm^{-2}, 120 min), we observed no signs of photodegradation as the absorption band of BODIPY remained during the irradiation process, which clearly confirms their resistance to photodegradation (Fig. S5, ESI†).

Encouraged by all of these findings, we next investigated the photocytotoxic activity of both sensitisers, **BOD-1** and **BOD-2**, against A549 human lung adenocarcinoma cell lines. We first studied the cellular localisation of **BOD-1** within A549 cells by using DAPI as a highly specific fluorescent dye to stain the nucleus. The fluorescence emission of **BOD-1** was strong enough for its visualisation in the cellular medium. Based on the counterstain and green fluorescence emitted from the cells, we concluded that **BOD-1** had localised in the cytosol (Fig. 4). Having confirmed that **BOD-1** passed efficiently through the cell membrane, we next investigated its photodynamic activity in A549 cells in both the absence and presence of light. First, the cell lines were loaded with increasingly greater doses of **BOD-1** (or **BOD-2**). One group of cells protected from light

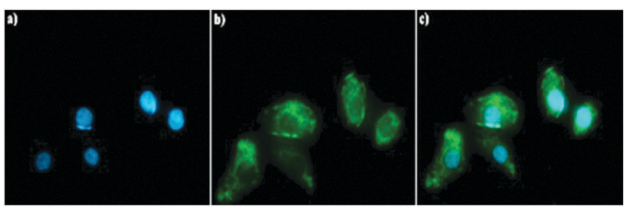

Fig. 4 Fluorescence images of human lung adenocarcinoma cells (A549). Fluorescence image of cells treated with (a) DAPI (control); (b) **BOD-1** (10 μM); (c) merged images of (a and b).

Published on 17 May 2021. Downloaded by Izmir Yuksek Teknoloji on 9/6/2022 2:34:58 PM.

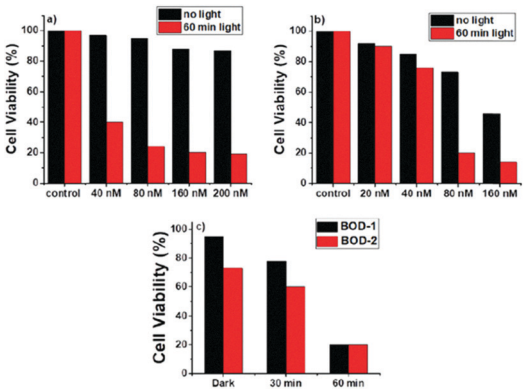

Fig. 5 Cell viability of A549 cells after treatment with (a) **BOD-1** and (b) **BOD-2** at different concentrations. The control group was incubated only with the cell culture medium. (c) Effect of light dose on cell viability (**BOD-1** and **BOD-2**, green LED, 525 nm, 3.3 W cm^{-2}, 80 nM).

throughout the incubation process showed relatively no decrease in cell viability up to 200 nM, thereby demonstrating the great cellular biocompatibility of the photosensitiser.[19] Another group of cell lines was irritated with green light at 525 nm at a fluence rate of 3.3 mW cm^{-2} for 60 min.

Based on the results of the MTT assay, in the cell lines illuminated by green light we observed a notable reduction in viability, even at very low concentrations of **BOD-1**, with an EC_{50} value of 20 nM (EC_{50} = 60 nM for **BOD-2**). Last, the effect of change in light dosage was assessed by treating cell lines with 80 nM of **BOD-1** and exposing them to light for 30 min. The results showed that the extent of light illumination was critical to the photosensitiser's photodynamic efficiency (Fig. 5c).

In conclusion, we reported a new generation of halogenated BODIPY-based photosensitisers, which demonstrated excellent photoactivity and photocytotoxicity both in solution and living cells. The significant increase in Φ_Δ confirms that incorporating bromine atoms into the vinyl backbone of a BODIPY skeleton was an efficient means to transform a non-active BODIPY dye into a highly active triplet sensitiser. The triplet excited state lifetimes of the photosensitisers were in the range of 101 to 145 μs. Significant upconversion was observed for **BOD-2** when combined with perylene as the triplet acceptor, with upconversion quantum yields up to 4.88%. The photosensitiser that we developed, **BOD-1**, was far more photoactive than the widely used 2, 6-dibromo BODIPY derivatives and relatively more emissive than their corresponding 2,6-diiodo analogues, thereby making it a highly promising tool for imaging-guided PDT.

Conflicts of interest

There are no conflicts to declare.

Notes and references

1 (*a*) D. E. J. G. J. Dolmans, D. Fukumura and R. K. Jain, *Nat. Rev. Cancer*, 2003, **3**, 380–387; (*b*) P. Babilas, S. Schreml, M. Landthaler and M. R. Szeimies, *Photodermatol., Photoimmunol. Photomed.*, 2010, **26**, 118–132; (*c*) M. Klausen, M. Ucuncu and M. Bradley, *Molecules*, 2020, **25**, 5239–5269.
2 P. Agostinis, K. Berg, K. A. Cengel, T. H. Foster, A. W. Girotti, S. O. Gollnick, S. M. Hahn, M. R. Hamblin, A. Juzeniene, D. Kessel, M. Korbelik, J. Moan, P. Mroz, D. Nowis, J. Piette, B. C. Wilson and J. Golab, *Ca-Cancer J. Clin.*, 2011, **61**, 250–281.
3 (*a*) R. Baskaran, J. Lee and S. Yang, *Biomater. Sci.*, 2018, **22**, 25–32; (*b*) Y. Lin, T. Zhou, R. Bai and Y. Xie, *J. Enzyme Inhib. Med. Chem.*, 2020, **35**, 1080–1099.
4 (*a*) S. G. Awuah and Y. You, *RSC Adv.*, 2012, **2**, 11169–11183; (*b*) A. Kamkaew, H. S. Lim, H. B. Lee, L. V. Kiew, L. Y. Chung and K. Burgess, *Chem. Soc. Rev.*, 2013, **42**, 77–88.
5 (*a*) A. Loudet and K. Burgess, *Chem. Rev.*, 2007, **107**, 4891–4932; (*b*) N. Boens, V. Leen and W. Dehaen, *Chem. Soc. Rev.*, 2012, **41**, 1130–1172.
6 (*a*) J. Zhao, W. Wu, J. Sun and S. Guo, *Chem. Soc. Rev.*, 2013, **42**, 5323–5351; (*b*) K. Chen, Y. Dong, X. Zhao, M. Imran, G. Tang, J. Zhao and Q. Liu, *Front. Chem.*, 2019, **7**, 821–834; (*c*) J. Zhao, K. Xu, W. Yang, Z. Wang and F. Zhong, *Chem. Soc. Rev.*, 2015, **44**, 8904–8939.
7 (*a*) X. Li, S. Kolemen, J. Yoon and E. U. Akkaya, *Adv. Funct. Mater.*, 2017, **27**, 1604053; (*b*) W. M. Gallagher, L. T. Allen, C. O'Shea, T. Kenna, M. Hall, A. Gorman, J. Killoran and D. F. O'Shea, *Br. J. Cancer*, 2005, **92**, 1702–1710; (*c*) T. Yogo, Y. Urano, Y. Ishitsuka, F. Maniwa and T. Nagano, *J. Am. Chem. Soc.*, 2005, **127**, 12162–12163; (*d*) W. Wu, X. Cui and J. Zhao, *Chem. Commun.*, 2013, **49**, 9009–9011; (*e*) S. H. Choi, K. Kim, J. Jeon, B. Meka, D. Bucella, K. Pang, S. Khatua, J. Lee and D. G. Churchill, *Inorg. Chem.*, 2008, **47**, 11071–11083; (*f*) X. F. Zhang and X. Yang, *J. Phys. Chem. B*, 2013, **117**, 5533–5539.
8 (*a*) P. Irmler, F. S. Gogesch, C. B. Larsen, O. S. Wenger and R. F. Winter, *Dalton Trans.*, 2019, **48**, 1171–1174; (*b*) M. Ucuncu, E. Karakus, E. D. Kurulgan, M. Sayar, S. Dartar and M. Emrullahoğlu, *Org. Lett.*, 2017, **19**, 2522–2525.
9 (*a*) M. A. Filatov, S. Karuthedath, P. M. Polestshuk, S. Callaghan, K. J. Flanagan, M. Telitchko, T. Wiesner, F. Laquai and M. O. Senge, *Chem. Phys.*, 2018, **20**, 8016–8031; (*b*) L. Huang, X. Yu, W. Wu and J. Zhao, *Org. Lett.*, 2012, **14**, 2594–2597.
10 (*a*) J. T. Buck, A. M. Boudreau, A. DeCarmine, R. W. Wilson, J. Hampsey and T. Mani, *Chemistry*, 2019, **5**, 138–155; (*b*) V. N. Nguyen, Y. Yim, S. Kim, B. Ryu, K. M. K. Swamy, G. Kim, N. Kwon, C. Y. Kim, S. Park and J. Yoon, *Angew. Chem., Int. Ed.*, 2020, **59**, 8957–8962.
11 T. Özdemir, J. L. Bila, F. Sözmen, L. T. Yıldırım and E. U. Akkaya, *Org. Lett.*, 2016, **18**, 4821–4823.
12 (*a*) J. Zou, Z. Yin, K. Ding, Q. Tang, J. Li, W. Si, J. Shao, Q. Zhang, W. Huang and X. Dong, *ACS Appl. Mater. Interfaces*, 2017, **9**, 32475–32481; (*b*) R. Lincoln, A. M. Durantini, K. E. Greene, S. R. Martinez, R. Konx, M. C. Becerra and G. Cosa, *Photochem. Photobiol. Sci.*, 2017, **16**, 178–184; (*c*) A. Turksoy, D. Yıldız and E. U. Akkaya, *Coord. Chem. Rev.*, 2017, **379**, 47–64; (*d*) C. S. Kue, S. Y. Ng, S. H. Voon, A. Kamkaew, L. Y. Chung, L. V. Kiew and H. B. Lee, *Photochem. Photobiol. Sci.*, 2018, **17**, 1691–1708.
13 V. C. Alejandro, F. P. Monica, A. P. Xelha, R. Mario, R. O. Gabriel, F. Norberto and R. G. Eva, *Polyhedron*, 2020, **176**, 114207.
14 R. Prietp-Montero, A. Pierto-Castaneda, R. Sola-LIano, A. R. Agarrabeitia, D. Garcia-Fresnadillo, I. Lopez-Arbeloa, A. Villanueva, M. J. Ortiz, S. Moya and V. Martinez-Martinez, *Photochem. Photobiol.*, 2020, **96**, 458–477.
15 (*a*) F. Ramirez, N. B. Desal and N. McKelvie, *J. Am. Chem. Soc.*, 1962, **84**, 1745–1747; (*b*) Y. Q. Fang, O. Lifchits and M. Lautens, *Synlett*, 2008, 413–417; (*c*) F. Legrand, K. Jouvin and G. Evano, *Isr. J. Chem.*, 2010, **50**, 588–604.
16 (*a*) S. Dartar, *MSc. Thesis*, İzmir Institute of Technology, 2019; (*b*) H. Ali, B. Guerin and J. E. Van Lier, *Dalton Trans.*, 2019, **48**, 11492–11507.
17 M. Gorbe, A. M. Costero, F. Sancenon, R. Martinez-Martinez, R. Ballesteros-Cillero, L. E. Ochando, K. Chulvi, R. Gotor and S. Gil, *Dyes Pigm.*, 2018, **160**, 198–207.
18 (*a*) T. N. Singh-Rachford, A. Haefele, R. Ziessel and F. N. Castellano, *J. Am. Chem. Soc.*, 2008, **130**, 16164–16165; (*b*) Z. Wang and J. Zhao, *Org. Lett.*, 2017, **19**, 4492–4495.
19 ESI†.

 This journal is © The Royal Society of Chemistry 2021